

## Description and outlook of the $^{50,53}\text{Cr}(\text{n},\gamma)$ cross section measurement at n\_TOF and HiSPANoS

P. Pérez-Maroto<sup>1</sup>, C. Guerrero<sup>1</sup>, A. Casanovas<sup>2</sup>, B. Fernández<sup>1</sup>, O. Aberle<sup>3</sup>, V. Alcayne<sup>4</sup>, S. Altieri<sup>5,6</sup>, S. Amaducci<sup>7</sup>, J. Andrzejewski<sup>8</sup>, V. Babiano-Suarez<sup>9</sup>, M. Bacak<sup>3</sup>, J. Balibrea Correa<sup>9</sup>, C. Beltrami<sup>5</sup>, S. Bennett<sup>10</sup>, A. P. Bernardes<sup>3</sup>, E. Berthoumieux<sup>11</sup>, R. Beyer<sup>12</sup>, M. Boromiza<sup>13</sup>, D. Bosnar<sup>14</sup>, M. Caamaño<sup>15</sup>, F. Calviño<sup>2</sup>, M. Calviani<sup>3</sup>, D. Cano-Ott<sup>4</sup>, D. M. Castelluccio<sup>16,17</sup>, F. Cerutti<sup>3</sup>, G. Cescutti<sup>18,19</sup>, S. Chasapoglou<sup>20</sup>, E. Chiaveri<sup>3,10</sup>, P. Colombetti<sup>21,22</sup>, N. Colonna<sup>23</sup>, P. Console Camprini<sup>17,16</sup>, G. Cortés<sup>2</sup>, M. A. Cortés-Giraldo<sup>1</sup>, L. Cosentino<sup>7</sup>, S. Cristallo<sup>24,25</sup>, S. Dellmann<sup>26</sup>, M. Di Castro<sup>3</sup>, S. Di Maria<sup>27</sup>, M. Diakaki<sup>20</sup>, M. Dietz<sup>28</sup>, C. Domingo-Pardo<sup>9</sup>, R. Dressler<sup>29</sup>, E. Dupont<sup>11</sup>, I. Durán<sup>15</sup>, Z. Eleme<sup>30</sup>, S. Fargier<sup>3</sup>, B. Fernández<sup>1</sup>, B. Fernández-Domínguez<sup>15</sup>, P. Finocchiaro<sup>7</sup>, S. Fiore<sup>16,31</sup>, V. Furman<sup>32</sup>, F. García-Infantes<sup>33,3</sup>, A. Gawlik-Ramiega<sup>8</sup>, G. Gervino<sup>21,22</sup>, S. Gilardoni<sup>3</sup>, E. González-Romero<sup>4</sup>, F. Gunsing<sup>11</sup>, C. Gustavino<sup>31</sup>, J. Heyse<sup>34</sup>, W. Hillman<sup>10</sup>, D. G. Jenkins<sup>35</sup>, E. Jericha<sup>36</sup>, A. Junghans<sup>12</sup>, Y. Kadi<sup>3</sup>, K. Kaperoni<sup>20</sup>, G. Kaur<sup>11</sup>, A. Kimura<sup>37</sup>, I. Knapová<sup>38</sup>, M. Kokkoris<sup>20</sup>, Y. Kopatch<sup>32</sup>, M. Krtička<sup>38</sup>, N. Kyritsis<sup>20</sup>, I. Ladarescu<sup>9</sup>, C. Lederer-Woods<sup>39</sup>, J. Lerendegui-Marco<sup>9</sup>, G. Lerner<sup>3</sup>, A. Manna<sup>17,40</sup>, T. Martínez<sup>4</sup>, A. Masi<sup>3</sup>, C. Massimi<sup>17,40</sup>, P. Mastinu<sup>41</sup>, M. Mastromarco<sup>23,42</sup>, E. A. Maugeri<sup>29</sup>, A. Mazzone<sup>23,43</sup>, E. Mendoza<sup>4</sup>, A. Mengoni<sup>16,17</sup>, V. Michalopoulou<sup>20</sup>, P. M. Milazzo<sup>18</sup>, R. Mucciola<sup>24,44</sup>, F. Murtas<sup>†45</sup>, E. Musacchio-Gonzalez<sup>41</sup>, A. Musumarra<sup>46,47</sup>, A. Negret<sup>13</sup>, A. Pérez de Rada<sup>4</sup>, N. Patronis<sup>30,3</sup>, J. A. Pavón-Rodríguez<sup>1,3</sup>, M. G. Pellegriti<sup>46</sup>, J. Perkowski<sup>8</sup>, C. Petrone<sup>13</sup>, E. Pirovano<sup>28</sup>, J. Plaza del Olmo<sup>4</sup>, S. Pomp<sup>48</sup>, I. Porras<sup>33</sup>, J. Praena<sup>33</sup>, J. M. Quesada<sup>1</sup>, R. Reifarth<sup>26</sup>, D. Rochman<sup>29</sup>, Y. Romanets<sup>27</sup>, C. Rubbia<sup>3</sup>, A. Sánchez-Caballero<sup>4</sup>, M. Sabaté-Gilarte<sup>3</sup>, P. Schillebeeckx<sup>34</sup>, D. Schumann<sup>29</sup>, A. Sekhar<sup>10</sup>, A. G. Smith<sup>10</sup>, N. V. Sosnin<sup>39</sup>, M. E. Stamatilis<sup>30,3</sup>, A. Sturniolo<sup>21</sup>, G. Tagliente<sup>23</sup>, A. Tarifeño-Saldivia<sup>2</sup>, D. Tarrío<sup>48</sup>, P. Torres-Sánchez<sup>33</sup>, E. Vagena<sup>30</sup>, S. Valenta<sup>38</sup>, V. Variale<sup>23</sup>, P. Vaz<sup>27</sup>, G. Vecchio<sup>7</sup>, D. Vescovi<sup>26</sup>, V. Vlachoudis<sup>3</sup>, R. Vlastou<sup>20</sup>, A. Wallner<sup>12</sup>, P. J. Woods<sup>39</sup>, T. Wright<sup>10</sup>, R. Zarrella<sup>17,40</sup>, P. Žugec<sup>14</sup>, and The n\_TOF Collaboration

<sup>1</sup>Universidad de Sevilla, Spain

<sup>2</sup>Universitat Politècnica de Catalunya, Spain

<sup>3</sup>European Organization for Nuclear Research (CERN), Switzerland

<sup>4</sup>Centro de Investigaciones Energéticas Medioambientales y Tecnológicas (CIEMAT), Spain

<sup>5</sup>Istituto Nazionale di Fisica Nucleare, Sezione di Pavia, Italy

<sup>6</sup>Department of Physics, University of Pavia, Italy

<sup>7</sup>INFN Laboratori Nazionali del Sud, Catania, Italy

<sup>8</sup>University of Lodz, Poland

<sup>9</sup>Instituto de Física Corpuscular, CSIC - Universidad de Valencia, Spain

<sup>10</sup>University of Manchester, United Kingdom

<sup>11</sup>CEA Irfu, Université Paris-Saclay, F-91191 Gif-sur-Yvette, France

<sup>12</sup>Helmholtz-Zentrum Dresden-Rossendorf, Germany

<sup>13</sup>Horia Hulubei National Institute of Physics and Nuclear Engineering, Romania

<sup>14</sup>Department of Physics, Faculty of Science, University of Zagreb, Zagreb, Croatia

<sup>15</sup>University of Santiago de Compostela, Spain

<sup>16</sup>Agenzia nazionale per le nuove tecnologie (ENEA), Italy<sup>17</sup>Istituto Nazionale di Fisica Nucleare, Sezione di Bologna, Italy<sup>18</sup>Istituto Nazionale di Fisica Nucleare, Sezione di Trieste, Italy<sup>19</sup>Department of Physics, University of Trieste, Italy<sup>20</sup>National Technical University of Athens, Greece<sup>21</sup>Istituto Nazionale di Fisica Nucleare, Sezione di Torino, Italy<sup>22</sup>Department of Physics, University of Torino, Italy<sup>23</sup>Istituto Nazionale di Fisica Nucleare, Sezione di Bari, Italy<sup>24</sup>Istituto Nazionale di Fisica Nucleare, Sezione di Perugia, Italy<sup>25</sup>Istituto Nazionale di Astrofisica - Osservatorio Astronomico di Teramo, Italy<sup>26</sup>Goethe University Frankfurt, Germany<sup>27</sup>Instituto Superior Técnico, Lisbon, Portugal<sup>28</sup>Physikalisch-Technische Bundesanstalt (PTB), Bundesallee 100, 38116 Braunschweig, Germany<sup>29</sup>Paul Scherrer Institut (PSI), Villigen, Switzerland<sup>30</sup>University of Ioannina, Greece<sup>31</sup>Istituto Nazionale di Fisica Nucleare, Sezione di Roma1, Roma, Italy<sup>32</sup>Affiliated with an institute covered by a cooperation agreement with CERN<sup>33</sup>University of Granada, Spain<sup>34</sup>European Commission, Joint Research Centre (JRC), Geel, Belgium<sup>35</sup>University of York, United Kingdom<sup>36</sup>TU Wien, Atominstirut, Stadionallee 2, 1020 Wien, Austria<sup>37</sup>Japan Atomic Energy Agency (JAEA), Tokai-Mura, Japan<sup>38</sup>Charles University, Prague, Czech Republic<sup>39</sup>School of Physics and Astronomy, University of Edinburgh, United Kingdom<sup>40</sup>Dipartimento di Fisica e Astronomia, Università di Bologna, Italy<sup>41</sup>INFN Laboratori Nazionali di Legnaro, Italy<sup>42</sup>Dipartimento Interateneo di Fisica, Università degli Studi di Bari, Italy<sup>43</sup>Consiglio Nazionale delle Ricerche, Bari, Italy<sup>44</sup>Dipartimento di Fisica e Geologia, Università di Perugia, Italy<sup>45</sup>INFN Laboratori Nazionali di Frascati, Italy<sup>46</sup>Istituto Nazionale di Fisica Nucleare, Sezione di Catania, Italy<sup>47</sup>Department of Physics and Astronomy, University of Catania, Italy<sup>48</sup>Department of Physics and Astronomy, Uppsala University, Box 516, 75120 Uppsala, Sweden

**Abstract.** Chromium is a very relevant element regarding criticality safety in nuclear reactors because of its presence in stainless steel, an important structural material. Currently, there are serious discrepancies between the different evaluations regarding the neutron capture cross sections of  $^{50}\text{Cr}$  and  $^{53}\text{Cr}$ , most probably related to the difficulty of reducing and then estimating the very large neutron scattering effects on the shape of the resonances. In this context, there is a recent entry in the Nuclear Energy Agency (NEA) High Priority Request List (HPRL) to measure these reactions between 1 and 100 keV with an accuracy of 8-10%. In response to this request, we have performed a time-of-flight experiment at CERN n\_TOF (Switzerland) and a complementary activation experiment on  $^{50}\text{Cr}$  at 30 and 90 keV at CNA HiSPANoS (Spain). The experiments are presented herein, together with a discussion on the quality of the preliminary data and the results to be expected.

## 1 Introduction and motivation

Nuclear criticality safety is among the main priorities nowadays regarding nuclear power [1]. As criticality safety aims at preventing an uncontrolled self-sustained nuclear chain reaction,

the knowledge of absorption cross sections in fuel elements and the structural materials is crucial for the calculations. In this context, the sizable abundance (11-26%) of chromium in stainless steel makes some criticality benchmarks that include large amounts of chromium (e.g., PU-MET-INTER-002 or HEU-COMP-INTER-005/4=KBR-15/Cr) very sensitive to its cross section, in particular capture on  $^{50}\text{Cr}$  and  $^{53}\text{Cr}$  [2, 3]. These criticality benchmarks show clearly that the current differences in the order of 30% between evaluations have a significant impact of about 1000 pcm in the corresponding criticality safety calculations. For this reason, considering that the differences in the evaluations are due to the limited accuracy of the current cross section data, the Nuclear Energy Agency (NEA) [4] included an entry in its High Priority Request List (HPRL) to measure the capture cross section of  $^{50}\text{Cr}$  and  $^{53}\text{Cr}$  between 1 and 100 keV with an accuracy of 8-10%.

There have been several measurements of this reaction in the past [5-9]. The aim of these measurements was, in general, to accumulate enough statistics up to a quite high neutron energy (several hundreds keV), hence the samples used were quite thick. Given the scattering-to-capture cross section ratio of about 300 in Cr isotopes, the associated multiple-scattering corrections (neutrons suffering one or more collisions inside the sample before being captured) are between 50% and 80% in previous experiments, which seems to be the reason behind the disagreement among them. It should also be mentioned that the majority of previous experiments did not employ low neutron sensitivity detectors to limit the effect of the large neutron scattering background.

In order to respond to the NEA-HPRL call, two experiments have been designed to overcome the issues of previous experiments. In the time-of-flight experiment, in addition to using low neutron sensitivity  $\text{C}_6\text{D}_6$  detectors, we have used (very) thin and “thick” samples to keep the neutron multiple-scattering to a minimum and still achieve, by measuring at the high neutron flux CERN n\_TOF-EAR1 facility [10, 11], enough statistics in the region up to 100 keV. This is complemented in the case of  $^{50}\text{Cr}$  by an activation measurement at CNA HiSPANoS [12] with quasi-Maxwellian neutron beams of 30 and 90 keV.

## 2 Time-of-Flight experiment at n\_TOF-EAR1

The n\_TOF facility has been in operation at CERN since 2001. The CERN Proton Synchrotron (CPS) sends 20 GeV/c proton pulses into a cylindrical lead target with a repetition rate of 0.8 Hz on average, producing neutrons by spallation. The neutrons are then moderated in borated water and travel 185 meters horizontally towards the EAR1 experimental area, 20 meters vertically towards EAR2 and 3 meters horizontally towards the NEAR station. The measurement presented herein was performed in EAR1 because of its superior energy resolution, which allows resolving resonances up to higher energies.

When the neutrons arrive to EAR1, after traversing the SiMon monitor [13], they impact in the sample, which is surrounded by four carbon fiber  $\text{C}_6\text{D}_6$  detectors [14] in order to observe the  $\gamma$ -rays cascades following neutron capture reactions.

The material of the samples was purchased to Trace Sciences International, consisting of fine powder of enriched  $\text{Cr}_2\text{O}_3$ , 94.6(4)% for  $^{50}\text{Cr}$  and 97.7(2)% for  $^{53}\text{Cr}$ . The powder was pressed into a 20 mm diameter PEEK capsule, achieving the thicknesses listed in Table 1. In addition, some auxiliary samples were also measured:  $^{nat}\text{Cr}$ , a dummy (PEEK capsule), empty and  $^{197}\text{Au}$ . A total number of  $4.6 \cdot 10^{18}$  protons impinged in the lead target during the 42 days of the experiment.

Cr is a relatively light nucleus and hence it features a very hard capture cascade, with a maximum  $\gamma$ -ray emission energy of 8.5 MeV for  $^{50}\text{Cr}$  and 9.7 MeV for  $^{53}\text{Cr}$ . This can be observed in Fig. 1, which shows the energy deposited spectra of the  $\gamma$ -cascade measured by the  $\text{C}_6\text{D}_6$  detectors for the thin samples of both isotopes. These energy spectra will be used

**Table 1.** Characteristics of the detectors and samples used in this work and in the previous measurements. The thicknesses have been minimized to reduce the multiple-scattering corrections while providing the necessary statistics in a reasonable beam time.

	Stieglitz (1971)	Beer (1975)	Kenny (1977)	Brusegan (1986)	Guber (2011)	Our work (2022)
(n,γ) detector	Liquid Sc.	Liquid Sc.	C <sub>6</sub> F <sub>6</sub>	C <sub>6</sub> D <sub>6</sub>	C <sub>6</sub> D <sub>6</sub>	C <sub>6</sub> D <sub>6</sub>
<sup>50</sup> Cr $n_{\text{at}}(10^{-3} \text{at/barn})$	8	18	5/8	7	-	0.6/1.9
<sup>53</sup> Cr $n_{\text{at}}(10^{-3} \text{at/barn})$	14	14	8/12	12/60	14	1.2/6.0

for validating the simulations of the detector response and the decay cascades necessary to implement the Pulse Height Weighting Technique (PHWT) [15].

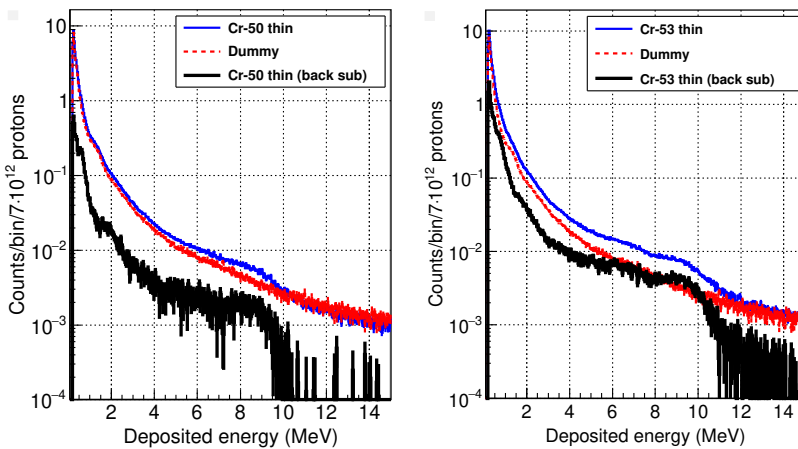


**Figure 1.** Deposited energy spectra of the <sup>50</sup>Cr thin sample (left) and the <sup>53</sup>Cr thin sample (right)  $\gamma$ -rays cascades on the C<sub>6</sub>D<sub>6</sub> detectors.

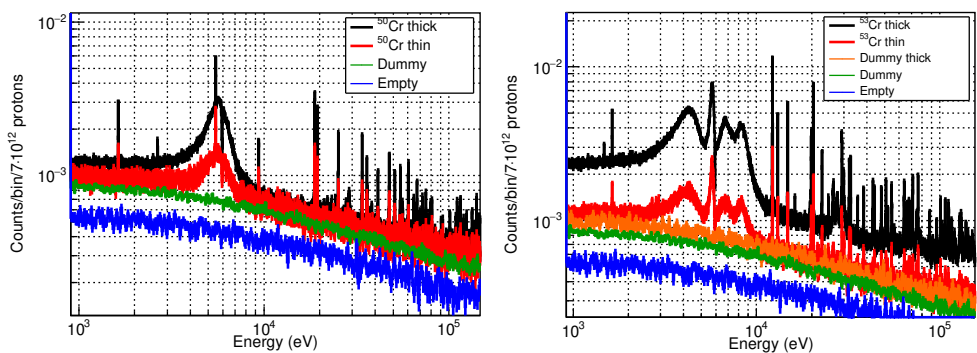


**Figure 2.** Counting rate per nominal proton pulse of <sup>50</sup>Cr (left) and <sup>53</sup>Cr (right), for both thin and thick samples. For the <sup>53</sup>Cr thick sample it was necessary to use a bigger capsule to fit all the material inside. The first resonance at 1.6 keV corresponds to <sup>52</sup>Cr, the main contaminant in the enriched samples.

The measured time-of-flight distributions for every Cr sample and the background measurements in the energy range of interest are displayed in Fig. 2. A difference in the background contribution and in the shape of the main resonance is visible between the thin and the thick sample, specially in  $^{53}\text{Cr}$  as it is the most massive sample. It is caused by neutron scattering, illustrating the importance of the thickness of the sample in this respect.

The capture data shows individual resonances with limited but enough statistics in the full energy range of interest, i.e. up to 100 keV. Having achieved this by means of very thin samples, it is expected that the quality and scope of the data will provide what is requested in the corresponding NEA HPRL entry.

### 3 $^{50}\text{Cr}$ activation at HiSPANoS

$^{51}\text{Cr}$  is an unstable isotope with  $T_{1/2}=27.7$  days, decaying by electron capture and emitting a 320.1 keV  $\gamma$ -ray ( $I_\gamma=9.91(1)\%$ ). This allows for a neutron activation measurement to obtain an integral cross section complementary to the time-of-flight experiment.

The MACS (Maxwellian Averaged Cross Section) of  $^{50}\text{Cr}$  has been measured at the HiSPANoS [12] facility at CNA [16]. A quasi-Maxwellian neutron spectrum (QMNS) with a temperature of 30 keV has been produced as usual via the  $^7\text{Li}(p,n)^7\text{Be}$  reaction with 1912 keV protons [17]. However, the energy range of interest goes up to 100 keV, but it is not straightforward to produce directly a high energy QMNS, for instance 90 keV. This has been achieved by a linear combination of different neutron spectra, none of them a QMNS, resulting from irradiation of a Li target with different proton energies, as proposed in Ref. [18]. In this case, we have produced a QMNS with 90 keV, which has also a high interest for s-process stellar nucleosynthesis [19], from the combination of irradiations with protons of 1912, 2040, 2080, 2120, 2150 and 2250 keV, resulting in the QMNS displayed in Fig. 3. The contribution of each spectrum has been chosen to minimize the difference between the SACS and the MACS<sub>90</sub> of  $^{197}\text{Au}$ . It is not the definitive choice as it might not be the most optimal one for the  $^{50}\text{Cr}$  cross section, with resonances at higher energies than  $^{197}\text{Au}$ . This is under investigation at the moment.

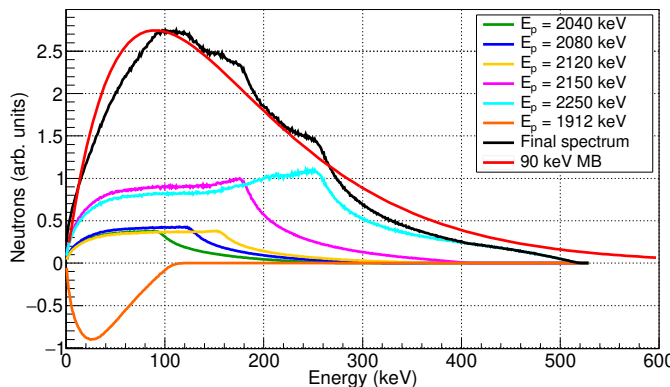


**Figure 3.** Quasi-Maxwellian 90 keV neutron spectrum produced with a combination of several spectra from different proton energies. These were obtained by simulating the  $^7\text{Li}(p,n)$  reaction with PINO.

The activation was performed at HiSPANoS, using the 3 MV Tandem Pelletron accelerator of CNA. A thick metallic Li target was inserted into an aluminum target holder with

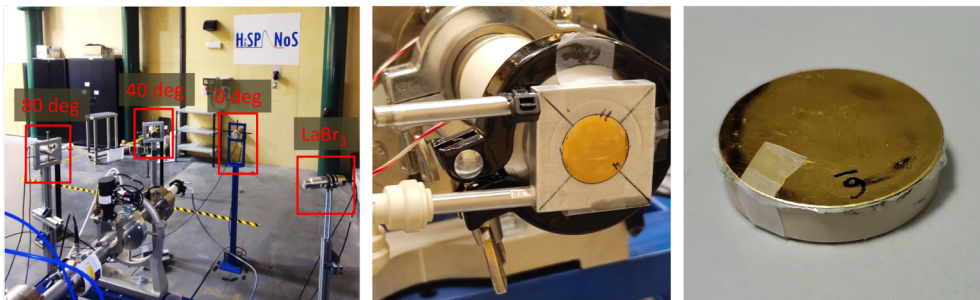


**Figure 4.** Experimental set-up for the activation measurement at HiSPANoS: (left)  $^6\text{Li}$ -glass detectors at three different angles to characterize the neutron spectra, along with a  $\text{LaBr}_3$  detector to measure the  $^7\text{Be}$  production, (center)  $^{197}\text{Au}$  sample at the face of the refrigerated aluminum target and (right)  $^{50}\text{Cr}$  sample with two gold foils on both sides.

a 500  $\mu\text{m}$  backing, similar to that reported in Ref. [20], that allows for water or air cooling, being the latter sufficient to avoid the melting of the Li target at the 6  $\mu\text{A}$  beam current applied.

The neutron spectrum produced by every proton energy used in the activation was characterized by time-of-flight with three  $^6\text{Li}$ -glass detectors placed at 0°, 40° and 80° (Fig. 4, left), at either 50 or 100 cm from the Li target. The measured spectra will be validated with PINO and SimLit-GEANT4 [21] simulations before the corresponding SACS and MACS values can be extracted from the ratios of activities of  $^{51}\text{Cr}$  (from  $^{50}\text{Cr}(\text{n},\gamma)$  reactions) and the references  $^{198}\text{Au}$  (from  $^{197}\text{Au}(\text{n},\gamma)$  reactions) and  $^7\text{Be}$  (from  $^7\text{Li}(\text{p},\text{n})$  reactions). A gold foil was activated alone for every proton energy (see Fig. 4, center), as an additional cross-check of the neutron spectra produced. All the activations were measured after each irradiation with a  $\text{LaBr}_3$  detector calibrated with radioactive sources complemented with GEANT4 simulations. The number of activated nuclei in each sample and the corresponding SACS and MACS are calculated using the procedure developed in Ref. [17].

The data analysis is still at a preliminary stage, but the analysis of a single  $^{197}\text{Au}$  foil under a QMNS of 30 keV has been almost completed. This simple case is meant as a validation, as the MACS of  $^{197}\text{Au}$  at 30 keV is a standard cross section [22]. Using the methodology mentioned above, we have obtained a preliminary  $\text{MACS}_{30}$  for  $^{197}\text{Au}$  of 600(23) mb. This result is already compatible within 3% and 2% with the values of 612(6) mb from KADONIS [18] and 620(11) mb from the standard cross section [22]. The nice agreement for  $^{197}\text{Au}$  allows to be optimistic about the results for  $^{50}\text{Cr}$ , for which the aimed accuracy is 8-10%.

## 4 Summary and conclusions

Chromium is quite abundant in stainless steel, used as a structural material in nuclear reactors. Criticality benchmarks show large sensitivity to Cr neutron capture, dominated by  $^{50,53}\text{Cr}$  between 1 and 100 keV, changing the criticality in the order of 1000 pcm for a 30% change in the cross section. The current evaluations have discrepancies of around 30%, a difference that is not reported or considered in the corresponding estimated uncertainties. The NEA opened an entry in its HPRL to measure these cross sections within 8 to 10% accuracy. As a response, a measurement of both isotopes was successfully performed at the n\_TOF facility at CERN. Because  $^{51}\text{Cr}$  is unstable, a complementary  $^{50}\text{Cr}$  activation measurement was performed at the HiSPANoS facility at CNA, with the aim to obtain the MACS at a temperature of  $kT = 30$

and 90 keV. The preliminary results from both experiments show high quality data, hence soon a new data set of  $^{50,53}\text{Cr}$  ( $n,\gamma$ ) cross sections will be released. Hopefully this new data set can be considered in forthcoming evaluations, contributing to reduce the uncertainty of safety calculations.

## Acknowledgements

These measurements have received funding from the Euroatom research and training programme 2014-2018 under grant agreement No 847594 (ARIEL), and from the Spanish national projects RTI2018-098117-B-C21 and PID2021-123879OB-C21.

## References

- [1] J.B. Briggs et al., Nuclear science and engineering **145**, 1 (2003)
- [2] V. Koscheev et al., *Use the results of measurements on KBR facility for testing of neutron data of main structural materials for fast reactors*, in *EPJ Web of Conferences* (EDP Sciences, 2017), Vol. 146, p. 06025
- [3] A. Trkov et al., Tech. rep. (2018)
- [4] Dupont, E. et al., EPJ Web Conf. **239**, 15005 (2020)
- [5] R. Stieglitz et al., Nuclear Physics A **163**, 592 (1971)
- [6] H. Beer, R.R. Spencer, Nuclear Physics A **240**, 29 (1975)
- [7] M. Kenny et al., *Neutron capture by the chromium isotopes* (Australian Atomic Energy Commission, 1977)
- [8] A. Brusegan et al., Radiation Effects **93**, 297 (1986)
- [9] K.H. Guber et al., Tech. rep., Oak Ridge National Lab.(ORNL), Oak Ridge, TN (United States) (2011)
- [10] C. Guerrero et al., The European Physical Journal A **49**, 1 (2013)
- [11] R. Esposito et al., Physical Review Accelerators and Beams **24**, 093001 (2021)
- [12] B. Fernández et al., *HiSPANoS facility and the new neutron beam line for TOF measurements at the Spanish National Accelerator Lab (CNA)*, in *Journal of Physics: Conference Series* (IOP Publishing, 2020), Vol. 1643, p. 012033
- [13] S. Marrone et al., Nucl. Instrum. Methods A **517**, 389 (2004)
- [14] R. Plag et al., Nucl. Instrum. Methods A **496**, 425 (2003)
- [15] U. Abbondanno et al., Nucl. Instrum. Methods A **521**, 454 (2004)
- [16] J. Gómez-Camacho et al., The European Physical Journal Plus **136**, 273 (2021)
- [17] W. Ratynski, F. Käppeler, Physical Review C **37**, 595 (1988)
- [18] R. Reifarth et al., The European Physical Journal Plus **133**, 424 (2018)
- [19] R. Käppeler et al., Reviews of Modern Physics **83**, 157 (2011)
- [20] J. Praena, P. Jiménez-Bonilla, *Two absolute integral measurements of the  $^{197}\text{Au}$  ( $n, \gamma$ ) stellar cross-section and solution of the historic discrepancies*, in *EPJ Web of Conferences* (EDP Sciences, 2020), Vol. 239, p. 19002
- [21] M. Friedman et al., Nucl. Instrum. Methods A **698**, 117 (2013)
- [22] A.D. Carlson et al., Nuclear Data Sheets **148**, 143 (2018)